X CONGRESSO NACIONAL DE ENGENHARIA MECÂNICA 2018
20 A 24 DE MAIO DE 2018 SALVADOR – BA – BRASIL

SIMULATING DYNAMIC SOIL-STRUCTURE INTERACTION USING THE DISCRETE ELEMENT METHOD

Marcelo Nery, marceloanery@gmail.com[1]
Euclides de Mesquita Neto, euclides@fem.unicamp.br[2]

[1] Dept. de Mec. Computacional, Faculdade de Engenharia Mecânica, Universidade Estadual de Campinas
[2] Dept. de Mec. Computacional, Faculdade de Engenharia Mecânica, Universidade Estadual de Campinas

This article describes a simulation of the Discret Element Method (DEM) applied to the transient analysis of Dynamic Soil-Structure Interaction (DSSI) problem. The soil particles, foundation and boundaries are composed by circular disks with different diameters. In the implemented algorithm the soil behavior is charatrerized compression-only constitutive equation. On the other hand, the interaction of the particles describing the foundation structure is characterized by a tension-compression constitutive equation. All particles that describes the boundaries of the soil domain are fixed not allowing either translational or rotational movements. All particles of the system have normal and tangential stiffness, damping properties as well as rolling resistance and dynamic friction coefficient between adjacent elements. Each particle may be given specific inertia properties. On all discrete elements, arbitrary external and gravitational forces, as well as displacements and velocities may be prescribed, except the boundaries elements. The resulting equations of motion are integrated using the Verlet scheme. In the presented simulations a sinusoidal external time load is applied on the foundation structure. The presented results included a validation strategy, a soil surface deformation curve for flexible and rigid foundations as well as the dynamic behavior of the foundation structure.

Keywords: *Particle Collision, Boundary Element Mehtod, Discrete Element Method, Dynamic Soil Structure Interaction*

1. INTRODUCTION

The Discrete Element Method (DEM) is a tool frequently used in the study of soil-structure interaction problems as well as to describe powder and granular materials that can be excited by dynamic or static loads. In DEM, soils and rocks are frequently modeled by 2D discs and 3D spheres, interacting with each other through a given set of mechanisms and laws.. DEM technique originally was introduced by "Cundall and Strack, 1979".

The DSSI analysis can be solved semi-analytically *"Carrion, et al, 2007"or* by making resort to a numerical discretization scheme such as the Boundary Element Method. Recently, some authors such as *"Gomes, 2014"* and *"Nery 2017"* have been solved dynamic and static problems using DEM and also coupling simulations of DEM with Finite Element Method (FEM).

According to "Sullivan, 2011", DEM can be applied to simulate physical laboratory tests where the evolution of all contact particles can be easily measured while it is hard to obtain this information in a physical laboratory test. Another advantage of apply DEM in simulation is the possibility it allows in analyzing systems where large, non-linear, displacements occur.

One important fact about DEM is the study of non-linear behavior of DSSI phenomena. Most of continuum models to describe DSSI problems only consider a continuum model with small linear displacements. DEM is able to model non-linear behavior which presents large displacements or large penetration along the time.

2. DISCRET ELEMENT METHOD

This work presents a dynamic interaction between the soil and a structure using on the Discrete Element Method (DEM), in which 2D disks were considered to model both soil and structure. The time integration algorithm also known as the Verlet "leapfrog algorithm" and presented by "*Sullivan, 2011*" is applied throughout the implementation.

An important fact about DEM is the contact search algorithm. Optimization of contact search algorithm can save computational efforts. In the implemented work, the contact search method was given by "*Munjiza, et al., 2012*". There are many algorithms for contact search and in the present implemented model the domain is divided in square cells with size of the biggest particle in the system *"Nery, 2018"*.

2.1. Equation of motion

The particles motions are governed by the following equations according to "*Nery, 2018*".

$$m_p \ddot{x}(t) = \sum_i F_i(t) \quad (1)$$

$$I_{p-gg} \ddot{\theta}(t) = \sum_i M_i(t) \quad (2)$$

In the equation of motion, the time (t) is discretized in time steps according to (1) and (2) motion equation, in which the linear degree of freedom (dof), x, and the rotational dof, θ are calculated.

The contact force that can be acting among the particles are normal and tangential elastic contact forces, denominated Fk_n and Fk_t, normal and tangential damping forces, denominated Fc_n and Fc_t and rolling resistance moment Mr. Gravitational forces may also be added to the forces acting on a particle as well as friction slip-stick contact condition.

The particle "p" studied in the equation (1) and (2) has mass m_p and mass inertia moment characterized by I_{p-gg} localized in the baricenter of the elements.

2.2. Acting Forces

The particles P1 and P2 have linear velocity V_p and tangential velocity ω_p according to the figure 1. A unit vector e_n connects the center of the particle P1 and P2. The tangential direction is designated by the unit tangential vector e_t.

When the particles are in contact, an overlap given by the quantity Δu can occur. For the tension-compression algorithm, Δu is calculated through the distance between the outer surfaces of the discs.

The implemented model can work just in compression model, figure 1a, or tension-compression model, figure 1a and 1.b. In the first case, fig. 1a, there only interaction forces if the particles present an overlap. In the second case, fig. 1b, there is a contact force even when the particles move away from each other.

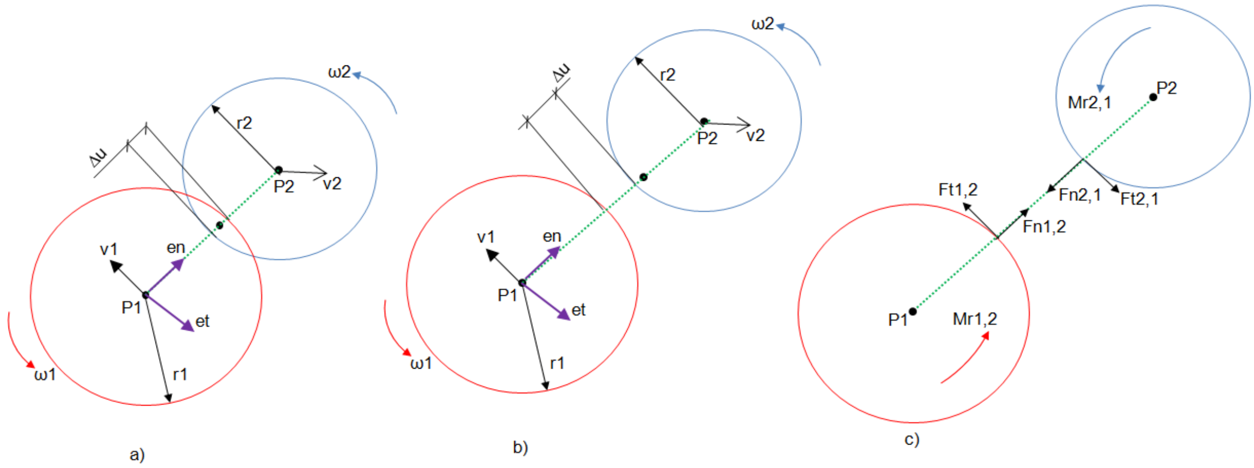

Figure 1. Particles geometry, a) with overlap, b) no overlap, c) Forces and moments

There are 6 constitutive parameters in the particles, denominated as: normal contact stiffness, k_n, normal damping viscosity, C_n, tangential contact stiffness, k_t, damping viscosity coefficient in the tangential direction, C_t, friction coefficient in the tangential direction, u_t, and the friction coefficient related to the rolling resistance, u_r. The possible particle contact models and constitutive parameters are shown in figure 2.

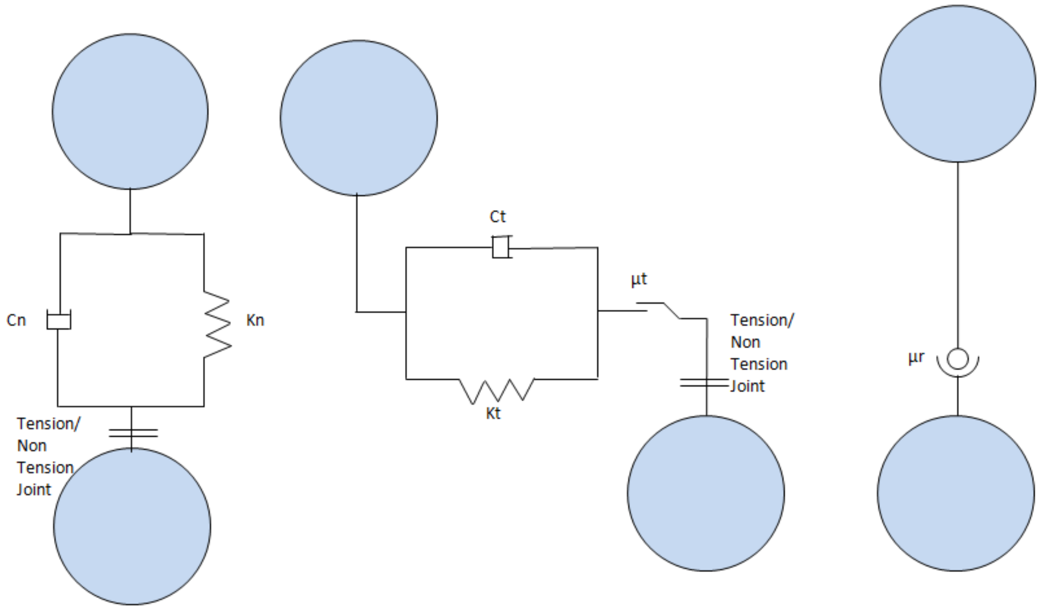

Figure 2. Model and constitutive parameters

2.3. Normal Contact Force

The normal contact force as described by "*Nery, 2018*", are decomposed in 2 components. Elastic component $\overline{F}_{kn}$ and damping component $\overline{F}_{cn}$.

$$\overline{F}_n = \overline{F}_{kn} + \overline{F}_{cn} \tag{3}$$

In which the elastic force $\overline{F}_{kn}$ is proportional to the overlap Δu and the stiffness normal component k_n:

$$\overline{F}_{kn} = k_n \, \Delta u \, \overline{e_n} \tag{4}$$

The damping normal force is given by:

$$\overline{F}_{cn} = -C_n \, \dot{x} \tag{5}$$

2.4. Tangential Contact Force

Similar to the normal force, the tangential force is composed by two components, elastic component $\overline{F}_{kt}$ and damping component, $\overline{F}_{ct}$, according to "*Onate e Rojek, 2004*".

$$\overline{Ft}_t = \overline{F}_{kt} + \overline{F}_{ct} \tag{6}$$

The stick/slip behavior of the tangential force is governed by the following slip condition:

$$\phi_t = \left|\overline{F}_{kt}\right| - \mu_t \, \overline{F}_n \tag{7}$$

2.5. Rolling Resistance Force

The rolling resistance model was described by "*Zhou, et al., 1999*" in which it's given by the normal force F_n, rolling radius R_r and friction rolling coefficient μ_r

$$M_r = \overline{F}_n \, R_r \, \mu_r \tag{8}$$

3. MODEL VALIDATION

3.1. Barrier Validation

This validation seeks to reproduce the problem simulated by "Li, *et al*., 2005" and validated by "*Nery*, *2018*". The original problem is shown in Figure 3. A box is filled with particles are accommodated into the domain under gravitational force over 2s, aiming the particle stabilization. In the sequence, the bottom starts to move up with the velocity 0,01m/s. The figure 4.a to 4.c show snapshots of the simulation process in different time steps, until 17s that is the end of the simulation. The applied time step was $\Delta t = 6\times10^{-5}$ s and the friction coefficients are μ_r =0,1 and μ_t = 0,4. The fixed boundary particles have $Db = 0{,}0025m$. The other used parameters are given in Table 1.

The reference solution simulated by "*Li*, *et al*., 2005" presents a final angle of the inclined plane formed by the particles with (21^0). The results simulated with DEM is in good agreement compared with the literature results according to figure 4c.

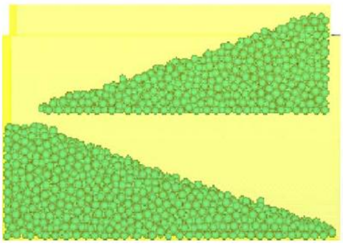

Figure 3. Barrier test

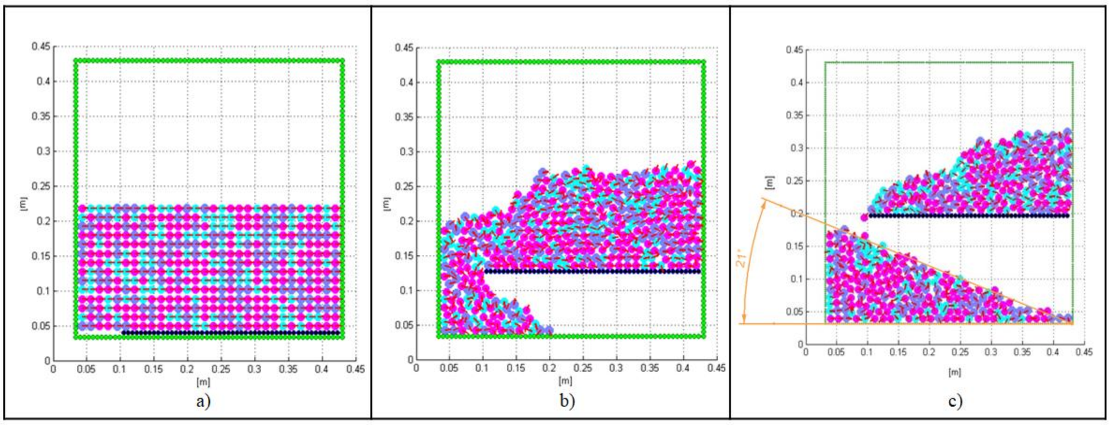

Figure 4: Barrier simulation, a) initial accommodation 2s, b) time step = 10s, c) final result 17s

The constitutive parameters used in this validation, are:

Table 1: Constitutive parameters

Parameters	Domain	Boundary	Barrier	Unit
k_n	$1{,}02\times10^6$	$6{,}5\times10^7$	$6{,}5\times10^7$	N/m
k_t	$5{,}09\times10^4$	$3{,}30\times10^7$	$3{,}30\times10^7$	N/m
C_n	173,4	1069	1069	N.s/m
C_t	27,7	1	1	N.s/m
ρ	2456	1056	1056	kg/m³

3.2. Comparison Between Continuum Theory and DEM

In order to compare solution of soil-structure given by the continuum theory with the proposed algorithm developed based on DEM, it's necessary to determine 2 constitutive parameters, namely Young's Modulus "E", Poisson coefficient ν (and/or shear modulus G_z) for the DEM particle ensemble. For this purpose the classic continuum mechanics equations (9) through (10) were used according to "*Nery, 2018*". The stress σ_z is given by the results of the external forces F_{ext} applied on the top particle layer and divided by the total transversal area of the top layer particles

A, strains ε_{xx} and ε_{yy} are calculated through the deformation components shown in the figure 5, where Df and Di is the final and initial pile height and Lf and Li the final and initial length

$$\sigma_z = \frac{Fext}{A} \qquad \varepsilon_{xx} = \frac{Df - Di}{Di} \qquad \varepsilon_{yy} = \frac{Lf - Li}{Li} \tag{9.a,b,c}$$

$$E = \frac{\sigma_z}{\varepsilon_{xx}} \qquad \nu = \frac{-\varepsilon_{yy}}{\varepsilon_{xx}} \qquad G_z = \frac{E}{2(1+\nu)} \tag{10.a,b,c}$$

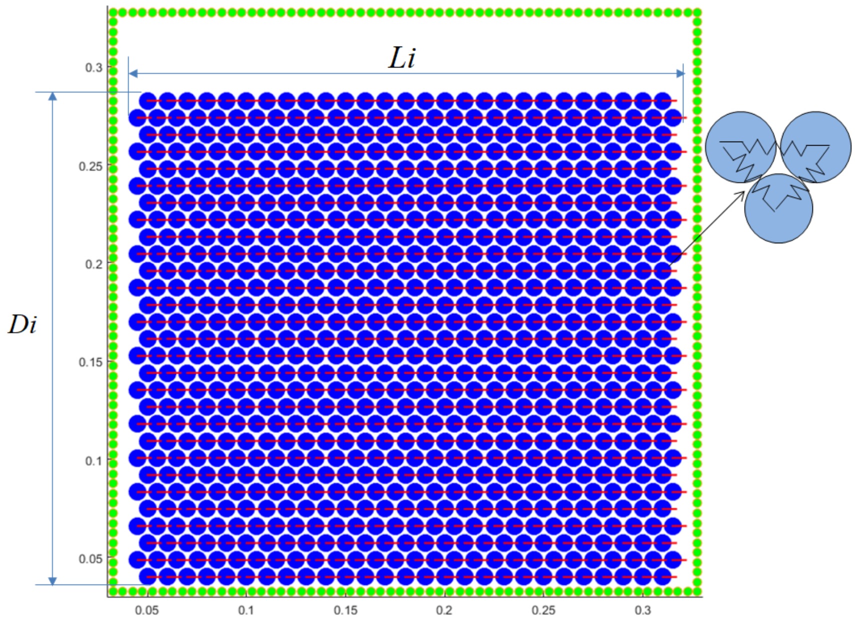

Figure 5: Boundary and soil particles system. Li=0,28[m] and Di=0,29[m]

The figure 6 presents the Poisson coefficient stabilization obtained through the different quantity of particles simulated. According to the results obtained in the simulation, then determined coefficient used in this study are ν=0,305, E=1,04 x 10^8 N/m² "*Nery, 2018*".

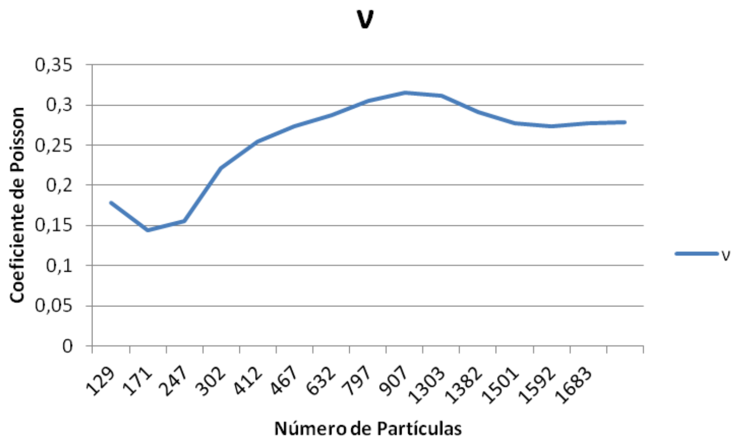

Figure 6: Poisson coefficient stabilization

After the determination of the soil constitutive parameters, as described above in this section, a first, static soil-structure interaction problem is solved using the DEM. A classical continuum description of a rigidless foundation interacting with the underlying soil is shown in figure 7a. The continuum based solution for the soil surface displacement due to an external vertical stress σ_z applied on the foundation is given by "*Poulos, 1974*" and reproduced in equation (11). Figure 7b shows the DEM model used to simulate this static soil structure interaction problem. The determination of the continuum constitutive parameters required for the solution (11), G_z and υ, was described in the previous paragraphs.

$$U_{z(x)} = \frac{-\sigma_z}{\pi . G_z (1-\nu^2)} \frac{af}{2} \left(\left(\left(1+\frac{x}{a_f}\right) Ln \left| 1+\frac{x}{a_f} \right| \right) + \left(\left(1-\frac{x}{a_f}\right) Ln \left(1+\frac{x}{a_f} \right) \right) \right) \tag{11}$$

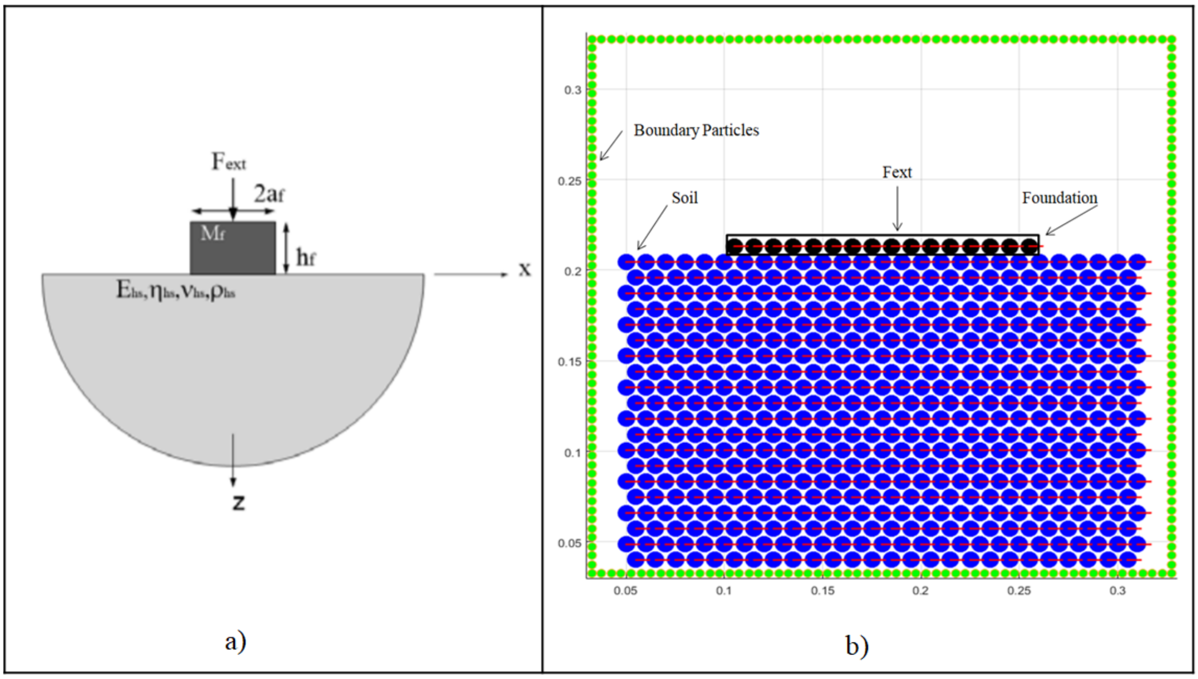

Figure 7: Foundation system. a) Continuum model, b) DEM model

The parameters used in the simulation of the figure (7b) are given in the table 2:

Table 2: Constitutive Parameters

Parameters	Soil	Boundary	Foundation	Unit
k_n	$1{,}8\times10^7$	$1{,}8x10^7$	$1{,}8x10^7$	N/m
k_t	$3{,}8x10^6$	$3{,}8x10^6$	$3{,}8x10^6$	N/m
C_n	150	200	150	N.s/m
C_t	27,7	27,7	1	N.s/m
Δt	$5x10^{-5}$	$5x10^{-5}$	$5x10^{-5}$	s
ρ	12105	0,4	0,4	kg/m³
μ_t	0,1	0,1	0,1	-
μ_r	0,1	0,1	0,1	-

The figure 8a presents a typical transient particle displacement behavior at the soil-foundation interface, due to a ‘ramp-like” external excitation, shown in figure 8b. Three distinct displacement phases can be recognized. Initially a gravitational load is applied to the particles and they vibrate until an accommodation patterns is found. After the particles have found an equilibrium position, the external loads (figure 8b) is applied. The soil surface displacement determined for two distinct levels of the vertical externa load (825N, 1650N) are shown, respectively in figures 8c and 8d. The analytical solution (11) is also shown. The results indicate clearly that the DEM, and this implementation in particular, is able to capture the static soil surface displacement.

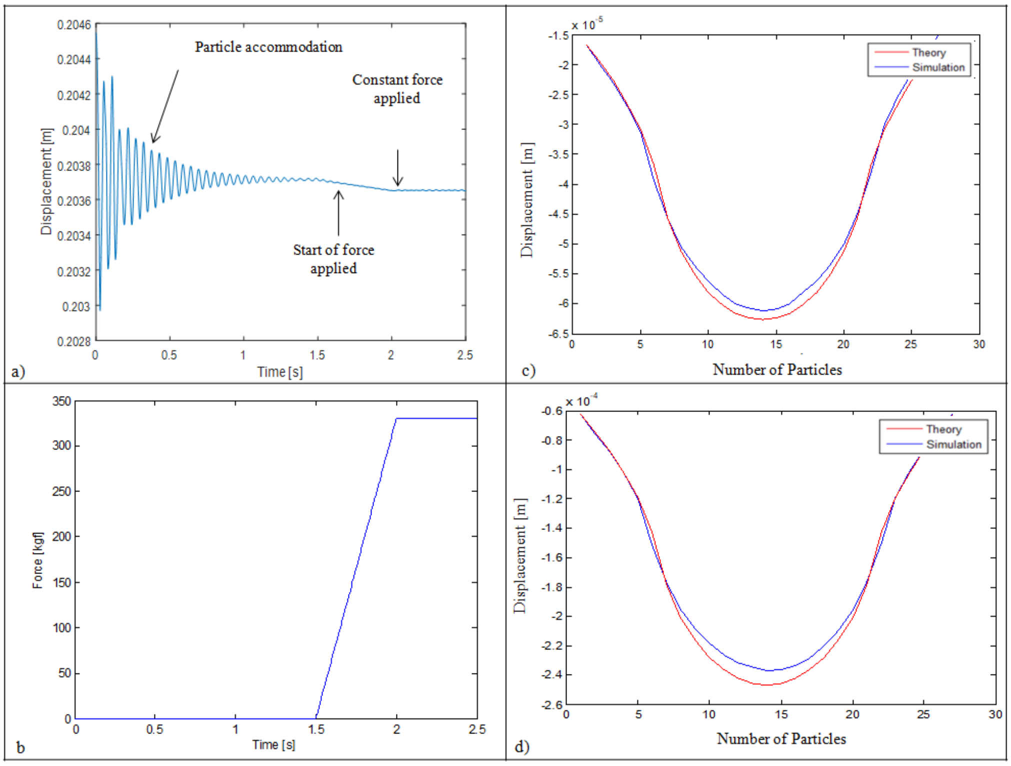

Figure 8: Theory x simulation convergence of a particle soil layer under foundation, a) transient particle displacement, b) applied external load, c) displacement result with 825N, d) displacement result with 1650N

4. NUMERICAL RESULTS

Since the DEM model is validated through the static solution of the continuum model, the article now investigates the dynamic response of a rigid foundation subjected to a sinusoidal external load F_{EXT}, as shown in figure 9. In the present simulation, the stiffness of the foundation is considered to be 20 higher than that of the underlying soil.

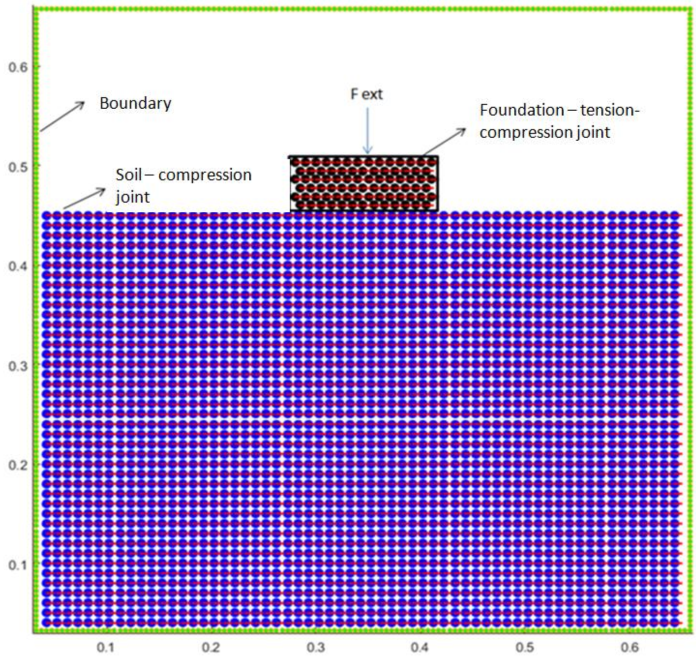

Figure 9: Dynamic model with stiff foundation

Initially the foundation was loaded by the same load pattern as shown in figure 8b, a ‘ramp-like’ load with intensity of 1650N. Constitutive parameters are shown in the table 3. The damping coefficient between the particles was set to a very small value. The typical transient displacement behavior of the foundation can be found in figure 10. The transient behavior of the foundation due to the applied load can be clearly recognized in the figure. The natural vibration frequency of the foundation over the soil layer is also clearly recognizable in the displacement response.

Table 3: Constitutive Parameters

Parameters	Soil	Boundary	Foundation	Unit
k_n	$9x10^5$	$1{,}8x10^7$	$1{,}8x10^7$	N/m
k_t	$1{,}9x19^5$	$3{,}8x10^6$	$3{,}8x10^6$	N/m
C_n	50	500	500	N.s/m
C_t	54	54	54	N.s/m
Δt	$3x10^{-5}$	$3x10^{-5}$	$3x10^{-5}$	s
ρ	12105	0,4	0,4	kg/m³
μ_t	0,1	0,1	0,1	-
μ_r	0,1	0,1	0,1	-

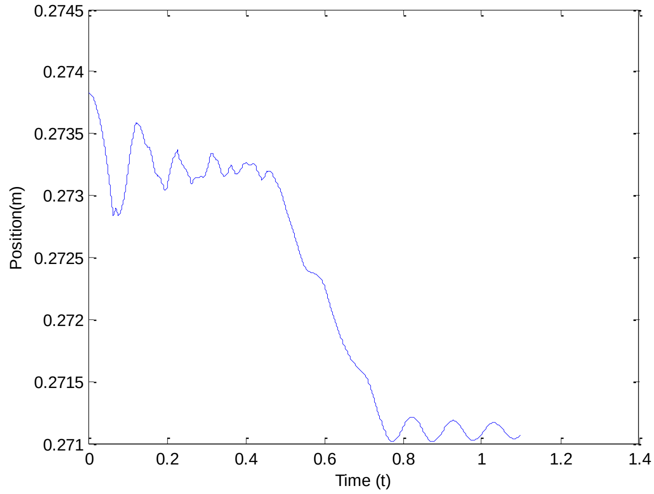

Figure 10: Displacement of a soil particle that is contact with foundation.

The natural vibration frequency is calculated in the equation (12).

$$\omega_n = \frac{1}{T} \tag{12}$$

The period T for the system represented in the figure (9) and table 3 for constitutive parameters, the calculated frequency is 9,6Hz. Figure 11 presents the elements of the top layer of the soil that is under the foundation. In this displacement solution, figure 11, the effect of the foundation rigidity can be recognized. This result should be compared to the case in which the foundation presents no rigidity and is shown in figures 8c and 8d.

Non-linear behavior due to a large excitation force. After the determination of the system natural vibration frequency, a new external sinusoidal force with a frequency 5 times smaller than the natural frequency is applied to the foundation. The force amplitude is 165 kgf according to the figure 12a.

The transient foundation displacement due to the external load is show in figure 12b. These snapshots of the foundation displacement are shown in figure 12c. These snapshots help to explain the displacement behavior shown in figure 12b. The excitation force is very large and as a result the foundation lifts up and disconnects from the soil surface-foundation interface, describes a trajectory in space as a rigid body and fall back on the soil, showing a partial contact at the soil-foundation interface. This is a very powerful result, showing the ability of the DEM to perform non-linear analysis. It is clearly not possible to obtain this kind of analysis and results using the continuum approach. The FEM can be used to simulate this problem but the mathematical formulation is much more complex and difficult to implement.

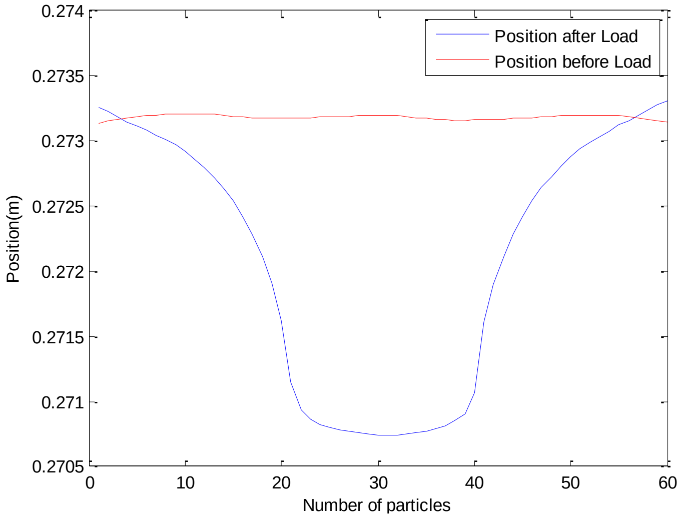

Figure 11. Top layer displacement of the soil

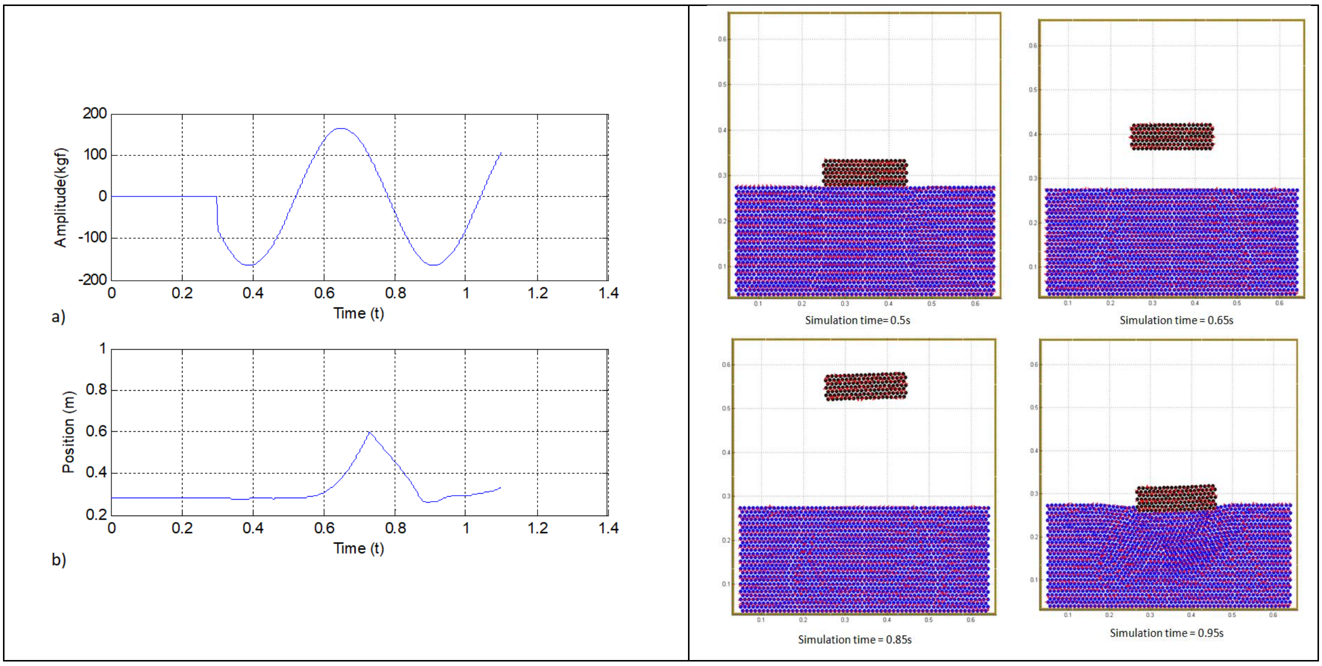

Figure 12. Particle behavior, a) load applied, b) displacement of a particle c) displacement snapshots

Small excitation – linear behavior. For the next example a small transient displacement of the foundation is aimed. The maximum foundation amplitude should be about 1% of the diameter of the soil particles. The new excitation pattern is shown in figure 13a. The frequency of the applied force is 1,92 Hz and 10x smaller than the natural frequency of the foundation. The transient foundation displacement is shown in figure 13b. Clearly there are 3 distinct phases for the foundation behavior. Up to the instant t<0.4s, the system is in the process of accommodation, due to applied gravity force. After the stabilizing the system, the sinusoidal force is applied at t=0.4s. The suddenly applied sinusoidal load induces a transient displacement with the frequency of the forced excitation overlaps with the first vertical natural frequency of the soil foundation system. This transient behavior lasts until approximately t=1.0s. After the transient effects have died out, the foundation vibrates with the frequency of the external excitation t>1.0s.

5. CONCLUDING REMARKS

A formulation and an implementation of the DEM has been presented and applied to describe the transient behavior of a soil-foundation system. The DEM implementation was validated by the solution of two distinct problems. In the sequence the foundation was excited by a large force inducing a strong non-linear response. This non-linear response includes foundation uplift and partial interface contact. A case for much smaller excitation induced a linear transient behavior with is compatible with the classical solution of a dynamic linear system. The presented results show the power of the DEM to model a series of linear and non-linear problems.

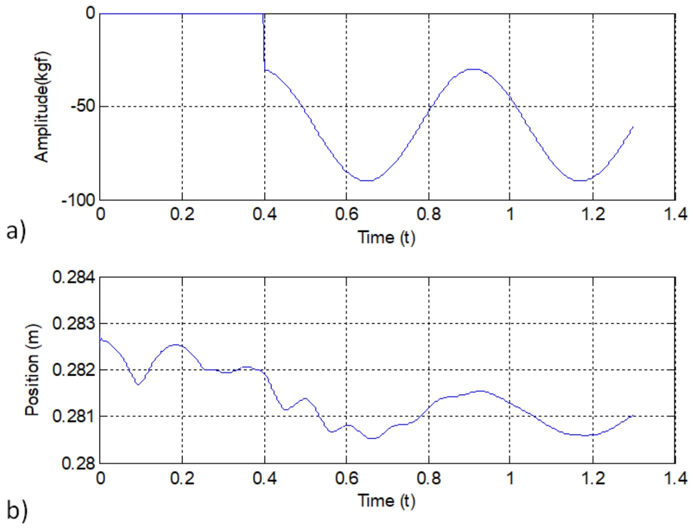

Figure 13. Linear particle behavior, a) load applied, b) displacement of a particle

6. ACKNOWLEDGEMENTS

The research leading to this work was funded by the São Paulo Research Foundation (Fapesp) through grants 2012/17948-4 and FAPESP CEPID Process 2013/08293-7. The support of Capes, CNPq and Faepex/Unicamp is also gratefully acknowledged

7. REFERENCES

Carrion, R, Amilcar, DOS, Mesquita, E, The influence of soil damping mechanisms and geo-profiles on the stationary response of 3D rigid block foundations. In Proceedings of the 19th Cobem, Brasília, 5-9 Novembro, 2007, pp. 01-10 (proceedings in CD-ROM).

Ai, J., Chen, J.F., Rotter, J.M, OOI, J.Y. Assessment of rolling resistance models in discrete element simulations. Powder Technology, v. 206, 269–282, 2011.

Munjiza, A., Andrews, K.R.F., Nbs contact detection algorithm for bodies of similar size. INTERNATIONAL Journal For Numerical Methods In Engineering, v. 43, 131–149, 1998.

Gomes, A.V.S., Estudo do acoplamento do Método dos Elementos Finitos e do Método dos Elementos Discretos na análise de interação solo – estrutura. 2014. Dissertação (Mestrado)- Faculdade de Engenharia Mecânica, Universidade Estadual de Campinas, Campinas. Orientador: Prof. Renato Pavanello (in Portuguese).

LI, Y., XU, Y., Thornton, C.A., A comparison of discrete element simulations and experiments for "sandpiles"composed of spherical particles. Powder Technology, v. 160, n. 3, 219 – 228, 2005.

Cundall, P.A, Strack, I.D.L, "A discrete numerical model for granular assemblies", *Geotechnique* 29, 47-65 (1979)

O'Sullivan, C. Particle discrete element modeling. Spon Press, 2011.

Onate, E, Rojek, J, Combination of discrete element and finite element methods for dynamic analysis of geomechanics problems. Computer Methods in Applied Mechanics and Engineering, v. 193, 3087–3128, 2004.

Zhou, Y., Wright, B., Yang, R., Xu, B, Yu, A., Rolling friction in the dynamic simulation of sandpile formation. Physica A: Statistical Mechanics and its Applications, v. 269, 536 – 553, 1999.

Poulos, H.G., Davis, E.H.: Elastic solutions for soil and rock mechanics, Wiley and Sons, NY, 1974

Nery, M.A.G., Aplicação do Método dos Elementos Discretos em Problemas da Interação Solo-Estruturas. Dissertação (Mestrado – Em elaboração) - Faculdade de Engenharia Mecânica, Universidade Estadual de Campinas, Campinas 2018. Orientador: Euclides Mesquita

Nery, Marcelo, Mesquita E.,: The Discrete Element Method (DEM) applied to Dynamic Soil-Structure Interaction. 24^{th} Cobem, Curitiba, 3-8 December 2017, Article 1321.

8. RESPONSABILITY NOTICE

The authors are the only responsible for the printed material included in this paper.